Chem Soc Rev

TUTORIAL REVIEW

View Article Online
View Journal | View Issue

Single molecule rotational probing of supercooled liquids

Cite this: *Chem. Soc. Rev.*, 2014, **43**, 977

Keewook Paeng and Laura J. Kaufman*

Much of the interesting behavior that has been observed in supercooled liquids appears to be related to dynamic heterogeneity, the presence of distinct dynamic environments – with no apparent underlying structural basis – in these systems. To most directly interrogate these environments, proposed to span regions just a few nanometers across, molecular length scale probes are required. Single molecule fluorescent microscopy was introduced to the field a decade ago and has provided strong evidence of dynamic heterogeneity in supercooled systems. However, only more recently has the full set of challenges associated with interpreting results of these experiments been described. With a fuller understanding of these challenges in hand, single molecule measurements can be employed to provide a more precise picture of dynamic heterogeneity in supercooled liquids and other complex systems. In this tutorial review, experimental and data analysis details are presented for the most commonly employed single molecule approach to studying supercooled liquids, the measurement of rotational dynamics of single molecule probes. Guidance is provided in experimental set-up and probe selection, with a focus on choices that affect data interpretation and probe sensitivity to dynamic heterogeneity.

Received 5th June 2013

DOI: 10.1039/c3cs60186b

www.rsc.org/csr

Key learning points

(1) Supercooled liquids show no apparent structural heterogeneity but do exhibit dynamic heterogeneity – the existence of distinct dynamical environments as a function of position and/or time.

(2) The potentially time-dependent relaxations of individual local environments in supercooled liquids may be studied through measuring rotational motion of embedded single molecule fluorophores. Such measurements may clarify results of ensemble measurements, which necessarily average over many environments, and thus provide a more precise picture of the length and time scales associated with dynamic heterogeneity.

(3) Probe choice is critical in single molecule rotational measurements of supercooled liquids: probes of sufficient photostability and appropriate size and relaxation dynamics must be chosen to allow for straightforward interpretation of the data.

I. Introduction

A liquid cooled below its melting temperature (T_m) that has avoided the first order phase transition to a crystalline solid is known as a supercooled liquid. Cooled further – to the glass transition temperature (T_g) and below – such systems are known as glasses. Glasses macroscopically behave like solids even while microscopically they appear to be nearly indistinguishable from normal liquids. This lack of structural distinction is especially striking in light of the stark dynamical distinction between a normal liquid and a glass: molecules at T_g may move more than 10 orders of magnitude slower than molecules in the liquid just above T_m.[1,2]

Department of Chemistry, Columbia University, New York, NY 10027, USA. E-mail: kaufman@chem.columbia.edu

A drive to understand the origin of the remarkable slowdown in dynamics that occurs in the supercooled regime in the absence of any clear structural changes has inspired much experimental and theoretical work. The introduction of the concept of dynamic heterogeneity has enriched understanding of glassy physics. Dynamic heterogeneity, also known as spatially heterogeneous dynamics or spatiotemporal heterogeneity, describes a situation in which molecules within the same system exhibit different dynamical behaviors as a function of time and/or space. For supercooled liquids, observations suggest – with a few notable exceptions[3,4] – that these differences emerge without any change in the static properties of the system, without an underlying structural basis for these different behaviors.[5,6] Because of the putative absence of a structural component, the heterogeneity in glassy systems is said to be purely dynamic. The causal relationship between dynamic heterogeneity and the abrupt slowing of

systems in the supercooled regime is not yet clear. To clarify how these phenomena are related as well as to enhance understanding of dynamic heterogeneity more broadly, much attention has been devoted to characterizing dynamic heterogeneity in supercooled liquids.

Experimentally, signatures of dynamic heterogeneity in supercooled liquids have been identified primarily through measurements monitoring molecular relaxations. In the frequency domain, dielectric spectroscopy has demonstrated the presence of a wide range of relaxation time scales in supercooled liquids. In the time domain, this broad frequency spread manifests as stretched exponential decays of correlation functions of various observables. Characterizing dynamic heterogeneity in more detail and understanding how it is causally related to the glass transition has been challenging, but a variety of experiments have measured quantities of interest in some supercooled liquids, including the size of regions of particularly slow dynamics and the time required for regions of slow dynamics to become fast.[5,6]

While some information about length and time scales associated with dynamic heterogeneity has been obtained from ensemble and sub-ensemble experiments, there is not yet broad agreement on these points, particularly with respect to the time scales on which distinct environments randomize, with experiments suggesting results spanning many orders of magnitude.[7,8] Probing dynamically distinct environments within supercooled liquids on an individual basis holds promise for revealing more details about dynamic heterogeneity. One of the key advantages of such a local approach is the ability to clarify the origin of the broad spectra measured in dielectric spectroscopy and the stretched exponential relaxations measured in time-domain approaches. Fig. 1 schematically depicts how single molecule experiments can clarify the origins of these dispersive relaxations. There are two limiting cases that are consistent with dynamic heterogeneity and the measurement of stretched exponential decays. In the first case (Fig. 1a), distinct environments persist for long times relative to the relaxation times of molecules within those environments. As a result, each region's relaxations will be exponential; however, the time scales of relaxation may differ, potentially by orders of magnitude. When summed, those exponential decays lead to a stretched exponential form. In the other limit (Fig. 1b), each environment probed yields the same stretched exponential decay as is seen for the ensemble, suggesting that distinct environments in these systems randomize on time scales no slower than the characteristic relaxation time measured in the ensemble. Between these limiting cases, stretched exponential relaxations may emerge when distinct environments exist for times that span the ensemble relaxation time of the system, potentially ranging from much shorter to much longer than the ensemble relaxation time. A system exhibiting this type of dynamic heterogeneity may have especially rich behavior, with – for example – anomalously fast (or slow) regions exhibiting unusually short (or long) persistence times compared to other regions of the sample.

More than ten years ago, the first experiment using single molecule fluorescent probes to interrogate a small molecule of supercooled liquid was reported.[9] In this study of rhodamine 6G embedded in *o*-terphenyl, rotational motion of the fluorescent

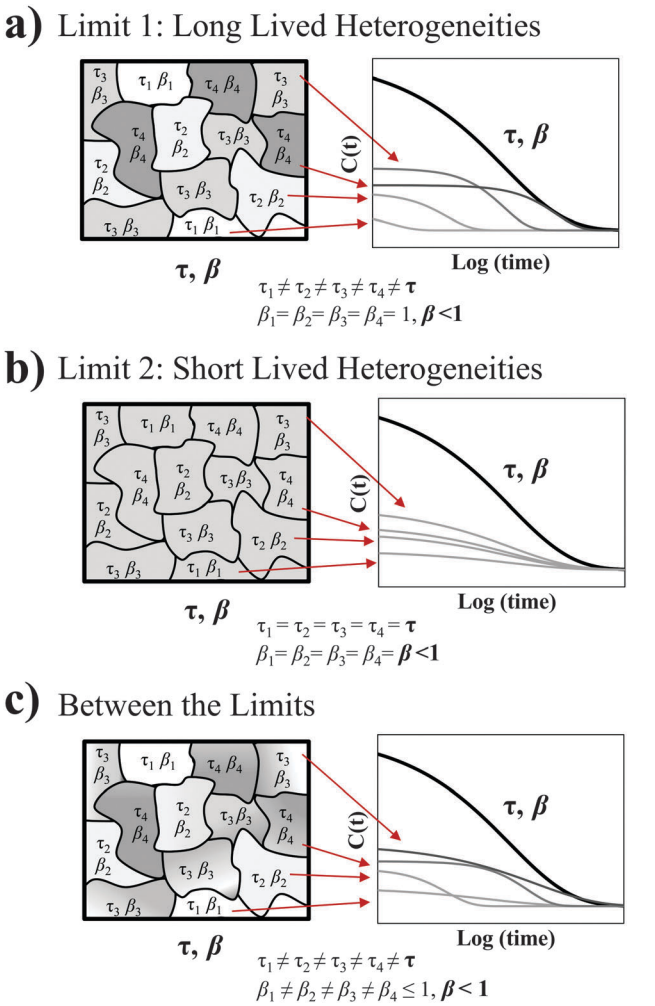

Fig. 1 Schematic illustration depicting how dynamic heterogeneity may contribute to dispersive relaxations and stretched exponential decays ($C(t) = \exp[-(t/\tau)^{\beta}]$ with $\beta < 1$). (a) Regions of distinct dynamics relax exponentially ($\beta = 1$), each with a different time scale, τ. This picture exists in the limit that dynamic changes occur on time scales much longer than the relaxation time of each region. (b) Each region within the sample displays the same relaxation dynamics, with the same stretching exponent ($\beta < 1$) and time scale. This picture suggests that distinct environments persist for times no longer than the ensemble relaxation time. (c) Distinct dynamic environments persist for time scales that span the ensemble relaxation time. Such a system will display some characteristics of both limiting scenarios depicted in (a) and (b).

probes was monitored. It was shown that individual probes in the same supercooled sample exhibited different characteristic relaxation times; moreover, there were indications that the given probe molecules experienced different dynamics over time. Subsequent studies have used similar approaches to directly demonstrate the presence of dynamic heterogeneity in both small molecule and polymeric supercooled liquids,[8–23] though challenges associated with interpreting the results of such experiments have also been recognized.[24] In spite of these practical challenges, experiments that can probe distinct environments in supercooled liquids hold promise for characterizing the distribution of different environments within them, the length scales and shapes of regions of particular dynamics, and the time scales

that govern the persistence of regions of particular dynamics within these systems.

Though various single molecule approaches to the study of supercooled liquids have been undertaken,[24,25] measurements of probe rotation have been most commonly employed. In this review, we discuss technical aspects of such measurements, with attention to how choices in experiment design and data analysis affect the information attainable from these experiments.

II. Experimental considerations

Experimental considerations presented here overlap with those of single molecule experiments in general, for which excellent reviews can be found on both technical and scientific issues.[26] In this tutorial review, we focus specifically on the experimental concerns most relevant to the study of single molecule probes embedded in supercooled liquids and glasses. While some single molecule experiments in supercooled liquids (particularly those in polymers) have measured single molecule probe fluorescence intensity and lifetime as a reporter of local host viscosity,[24,25] we describe here only the most commonly performed single molecule experiments in small molecule supercooled liquids, those in which the key observable is probe mobility as a reporter of local host dynamics and dynamic heterogeneity. While most experiments to date have measured probe rotational mobility, the considerations discussed here are also relevant for measurements of probe translational mobility.

A. Optical setup overview

Far field optical fluorescence microscopy has been widely employed for single molecule studies of supercooled liquids and glasses.[24,25] Both wide-field[10,14,17,18,21–23] and confocal[8,9,12,13,15,16,19,20] configurations have been employed. The prime advantage of the wide-field approach is that it enables study of multiple probe molecules simultaneously, providing easier access to distributions of properties of interest. On the other hand, a confocal approach has the merit of higher signal-to-noise since it limits background noise from sample regions outside the confocal volume. Total internal reflection microscopy, an approach commonly used in biological single molecule experiments, combines advantages of wide-field and confocal approaches as it allows detection of multiple probes simultaneously while limiting the background noise through the use of an evanescent field. This approach is impractical for supercooled liquids for a number of reasons including the requirement of a high numerical aperture (NA) objective and an interrogated medium with a low refractive index.[26]

Fig. 2 shows the schematics of typical wide-field and confocal set-ups used in single molecule experiments of supercooled liquids. Both set-ups are designed to excite and collect fluorescence from single molecule probes. A continuous wave laser is typically employed as the excitation source. To assure excitation of all probes regardless of their orientation, several approaches have been implemented. First, circularly polarized light may be used.[9,12,18,19] To compensate for reflection modulation of differently polarized light by the dichroic mirror, rather than use a single quarter waveplate, the combination of a quarter and half waveplate is used. Alternate approaches to exciting probes of all orientations in the sample plane include combining light of two orthogonal polarizations[23] or switching two orthogonal polarizations at high frequency relative to time scales of interest using an electro-optic modulator (EOM)[8,14,17] (Fig. 2a, dashed rectangles).

For a confocal approach (Fig. 2b), a telescope consisting of two lenses (L1, L2) is used to overfill the back aperture of the objective with a collimated beam. This is delivered to an objective lens to produce a tightly focused, diffraction limited excitation volume in the sample, with probe concentration chosen such that no more than one probe is typically present in the confocal volume. The confocal volume depends on the wavelength of excitation light and the NA of the objective lens. A typical confocal volume is $\approx 1\ \mu m^3$ for optical excitation.

For a wide-field approach (Fig. 2a), a telescope is used to set desired excitation beam size, and a third lens (L3) is used to focus light to the back of the objective lens, at the image plane. The size of the expanded beam, the focal length of the focusing lens, and the NA of the objective lens determine the size of the excited field of view. In the wide-field approach, an excitation intensity gradient along the field of view is typically present, with a Gaussian profile with the maximum at the center of the field of view. The excitation beam can be expanded and cropped to improve the homogeneity of the illuminated field. Greater homogeneity can be achieved by coupling the excitation laser into a multimode optical fiber that scrambles the transverse mode of the laser, as well as its polarization. This produces a random speckle pattern. Physically shaking the optical fiber using a piezoelectric buzzer spatially averages the speckle pattern, producing an evenly distributed intensity across the field of view (Fig. 2a, solid rectangle).[23]

After excitation, for both confocal and wide-field approaches, fluorescence passes through a dichroic mirror, is set to an appropriate size using a lens pair, and is additionally filtered using longpass and/or bandpass filters to eliminate reflected excitation light and spectral noise. In the confocal approach, the fluorescence signal that passes through the dichroic mirror is spatially filtered with a pinhole that rejects fluorescence from outside the confocal volume. A polarizing beam splitter separates the signal into two orthogonal polarizations. In the wide-field approach, this is typically a Wollaston prism, which separates orthogonally polarized light by an angle of ≈ 15 to 45°. The signals are then focused onto the detector(s), avalanche photodiodes for the confocal approach and an enhanced CCD camera in the wide-field approach. In the confocal approach, a piezostage can be used to scan over the sample to find probe molecules as well as to construct an image.

The acquisition of two orthogonal polarizations of fluorescent light from the probes assures collection of sufficient information to map probe rotation in the plane of the sample. There have also been configurations described and implemented that allow measurement of three dimensional probe orientation through analysis of the emission patterns formed by probes in defocused images.[24] While this approach provides complete orientational information, a relatively high signal-to-noise ratio is required to extract this information, which may lead to short trajectories that

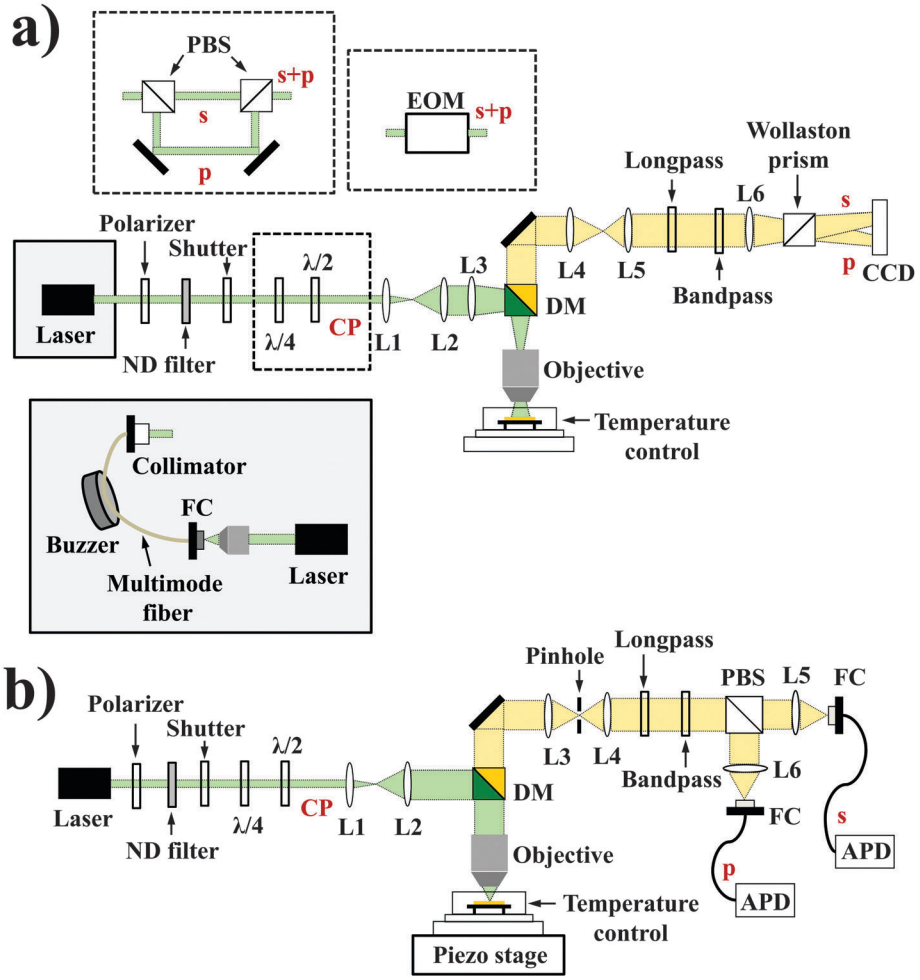

Fig. 2 Schematic diagrams of (a) wide-field and (b) confocal fluorescence microscope configurations appropriate for measurement of rotational dynamics of SM fluorescent probes in supercooled liquids. In the wide-field schematic, the inset rectangles indicate additional choices for (solid lines) creating a homogeneous field of view and (dashed lines) setting excitation polarization as described in the text. The choices for polarization are also relevant in the confocal approach. In this figure, s and p indicate orthogonal polarizations, and CP is circular polarization. Optical elements are abbreviated as follows: ND, neutral density filter; $\lambda/2$ ($\lambda/4$), half- (quarter-) waveplate; L, lens; DM, dichroic mirror; PBS, polarizing beam splitter; APD, avalanche photodiode; CCD, charge coupled device camera; EOM, electro-optic modulator; FC, fiber coupling.

contribute to challenges in interpreting rotational single molecule data (see Section V).

The wide-field approach can be used to monitor not only probe rotational motion but also probe translational motion. Here, a spectrally filtered image can be focused directly onto the detector without separating the signal into orthogonal polarizations. For translational monitoring, magnification beyond that generally appropriate for rotational single molecule measurements may be preferred. This is because monitoring translations of typical single molecule probes over accessible time scales is likely to require sub-diffraction localization, for which accuracy and precision are sensitively tied to detection details.[27] Details of some key aspects of the overall optical set-up as well as sample preparation and probe choice are described below.

B. Objective lens

Objective lenses used in single molecule experiments are typically 60–100× magnification with an NA of 0.7–1.4, with the lower NA objectives used for situations in which long working distances are required. NA is directly related to the collection angle by NA = $n\cdot\sin(\varphi)$, with n the index of refraction of the medium and φ the half-angle of the maximum cone of light that can enter or exit the lens. The collection efficiency is approximately 31% for an oil immersion objective with an NA of 1.4 and 14% for a long working distance air objective with an NA of 0.7.[28] Unfortunately, high NA objectives have short working distances and thus require sample configurations that may not be appropriate for single molecule experiments in supercooled liquids due to environmental control requirements. Indeed, to achieve stable temperature control over a relatively wide range of temperatures and to simultaneously enhance photostability of fluorescent probes, performing single molecule experiments in a vacuum cryostat is preferred (see Section IIC). Isolation of the sample within such a cryostat requires use of a long working distance air objective. In addition to limiting the proportion of emitted photons collected, the use of such low NA objectives may complicate interpretation of

the collected signals, such that non-exponential correlation functions may be obtained even for probes experiencing a homogeneous rotation.[13,29,30] This deviation from exponentiality is not a significant factor as long as objectives with NA > 0.6 are employed.[30]

C. Temperature control

Experimental configurations in which the sample is contained in a vacuum cryostat are preferred for several reasons. Because supercooled liquids experience dynamics that slow abruptly with decreasing temperature near T_g, the time scales of interest are long, requiring long time monitoring of individual probes. Indeed, host molecule structural relaxation times are $\approx$100 s at T_g. For single molecule probes, which are typically larger and rotating more slowly than the host molecules, the times required to characterize rotations are longer than those required to characterize host rotations, by up to several orders of magnitude. Because the time scales interrogated in these studies are quite different from those probed in most single molecule studies, single molecule experiments in supercooled liquids require special attention to physical and temperature stability.

Temperature control is also important in the single molecule study of supercooled liquids for other reasons. Unlike biological systems, where the physiologically relevant temperature range is narrow and close to room temperature, the temperature range of interest for glass forming liquids is wide and varies significantly across supercooled liquids. The two most well-studied low molecular weight glass formers – glycerol and *o*-terphenyl – have T_g values of 190 K and 243 K, respectively, while most polymeric glass formers have T_g values ranging from 200 to 500 K.[31] Beyond the wide range of temperatures that are of potential interest, sample temperature accuracy and stability are crucial in the study of glass formers since dynamics are very sensitive to temperature changes near T_g. For instance, in some glass formers, a change of 3–4 K can lead to an order of magnitude change in system dynamics.

The most common robust method to control sample temperature is through the use of a vacuum cryostat. A vacuum environment provides excellent thermal insulation. It also typically increases photostability of the fluorescent probes by reducing oxygen, since photobleaching events are often caused by reactions between excited fluorescent probes and triplet oxygen. On the other hand, introducing a vacuum cryostat reduces fluorescence collection efficiency. Generally, optical windows used in vacuum cryostats have thickness of 0.3–0.5 mm, introducing additional scattering and preventing the use of high NA objectives. In such configurations, long working distance objective lenses with NA of 0.7–0.8 are used. As described above, this decreases collection efficiency by a factor of $\approx$2 relative to the highest NA objectives available. Although it is not easy to implement, stable and accurate temperature control can be achieved with greater collection efficiency by inserting an air objective lens (available at NA up to 0.95) within the vacuum cryostat.[8]

D. Sample preparation

The purity of the sample – a requirement for near optical transparency – is critical in single molecule studies. The fluorescent probe concentrations used in these studies are on the order of 10^{-9} M, which sets an upper bound on fluorescent impurities allowed in the sample. Traditional purification methods such as re-crystallization and distillation are commonly used to clean the host sample. However, in many cases, removing fluorescent impurities through these approaches to less than a part per billion is quite challenging. One alternative and efficient way of achieving adequate optical transparency is through photobleaching fluorescent impurities. This can be achieved in a variety of ways, including the use of a low cost $\approx$10 W setup based on LEDs[32] or by placing the host sample in the path of a laser of similar power.

Additional sample characteristics also affect the ultimate signal to noise ratio in single molecule experiments in supercooled liquids. For the wide-field approach, thin samples are desirable since fluorescence from the whole thickness of the sample is collected. However, de-wetting of samples occurs more readily for thinner samples, especially for glass formers of low molecular weight. In addition, interfacial effects near both sample–substrate and sample–air interfaces may result in dynamics in these regions that are distinct from those in the bulk.[33] To best balance these competing effects, samples of 100–300 nm thickness are preferred. We note that for samples of such thickness, differences between signal-to-noise in wide-field and confocal approaches will be less significant for samples thicker than the axial dimension of the confocal volume.

E. Probe choice

As in all single molecule experiments, choice of probe is an important factor allowing for the success of a given experiment. In supercooled liquids, single molecule probe choice not only determines the viability of the experiment but also strongly influences the information content of the measured data. Thus, for measurements in supercooled liquids, choice of probe is critical. *Indeed, almost all observables relevant to the study of dynamic heterogeneity strongly depend on the selection of the fluorescent probe.* The characteristics of probes that most strongly affect the measurements are probe photostability and probe size. The effects of these factors on measurements are introduced here and discussed in more detail in Section V.

For all single molecule fluorescence experiments, probes with high extinction coefficient and quantum yield are necessary. Extinction coefficient generally increases with molecule size, thus encouraging use of large molecules. High quantum yield is typically found in rigid molecules, which when excited tend to have fewer non-radiative decay pathways. Moreover, for absorption in the visible region, molecules with a relatively small energy gap between the ground and excited electronic states are required. Overall, this leads to the choice of single molecule fluorophores that are large, conjugated, and rigid.[26] Additionally, many supercooled liquids are non-polar; to best mimic host intermolecular interactions between the probe and host, uncharged and relatively non-polar probes are preferred in such cases. Rigid and/or non-polar molecules tend to have small Stokes shifts, as no large charge distribution rearrangements occur upon excitation. For single molecule experiments in supercooled liquids, rhodamine 6G (R6G) and

perylene dicarboximide (PDI) probes have been most commonly employed.[8–10,15,17,18,23]

Both R6G and PDI have Stokes shifts of <20 nm, with appreciably overlapping absorption and emission bands. When fluorescent probes have spectra with significant overlap, selection of filters becomes an important consideration. The most efficient and flexible setup for separating fluorescent signal from spectral noise and elastic scattering from the excitation laser utilizes a dichroic mirror and longpass filter with steep cutoff transitions close to the excitation line. Currently filters with cutoff transition width as narrow as 100 cm^{-1} (≈ 3 nm in the green excitation range) with a transmission efficiency of over 95% are available. The spectral properties of the particular set of filters used for PDI probes employed in our work are shown in Fig. 3. Depending on the spectral characteristics of the chosen fluorescent probe in a specific host, 30–70% of the fluorescent signal may be lost to spectral filtering following emission.

A single molecule probe selected for the photophysical properties detailed above may still not be suitable for use in single molecule experiments if its photostability is poor, particularly if it is prone to photobleaching. While the tendency of a fluorophore to photobleach may be minimized by reducing oxygen in the environment as is done through use of a vacuum cryostat, all fluorophores eventually undergo irreversible changes that render them non-fluorescent. The number of cycles of excitation and emission that a probe can undergo before photobleaching is a crucial consideration for single molecule experiments in supercooled liquids, as a limited trajectory length introduces complications in identifying and characterizing dynamic heterogeneity.[24,34–36] While employing lower laser powers can extend time to photobleaching, this may require longer time-averaging to achieve an acceptable signal-to-noise ratio, offsetting enhanced time to photobleaching. In practice, laser power densities of ≈ 10 μW μm^{-2} have been used in both wide-field and confocal single molecule experiments in supercooled liquids, and trajectory lengths have typically been a few thousand seconds. In these measurements, the trajectory length relative to the rotational relaxation time of the probe is the most relevant time scale, as this determines how accurately and precisely rotational motion of the probe can be characterized. Trajectories of 10–1500 τ_c, with τ_c the rotational correlation time of the probe have been reported.[8–10,15,17,18,23]

While the trajectory length in terms of the rotational correlation time of the probe is of outmost importance in accurately determining the rotational rate of the probe, it is probe rotational rate relative to host rotational dynamics that sets the sensitivity of the probe to changes in host dynamics over time. Similarly, probe size relative to size of regions of distinct dynamics in the host sets the sensitivity of the probe to variability in host dynamics in space. A probe that is significantly slower and/or larger than the host molecules may be unable to report dynamic heterogeneity in the host, instead reporting an average of the different environments it experiences in time and/or space.

Balancing the competing requirements for probe photophysical characteristics, which generally improve with increasing probe size, and for probe ability to sensitively report dynamic heterogeneity, which deteriorates with increasing probe size, has been the primary challenge in single molecule experiments in supercooled liquids.

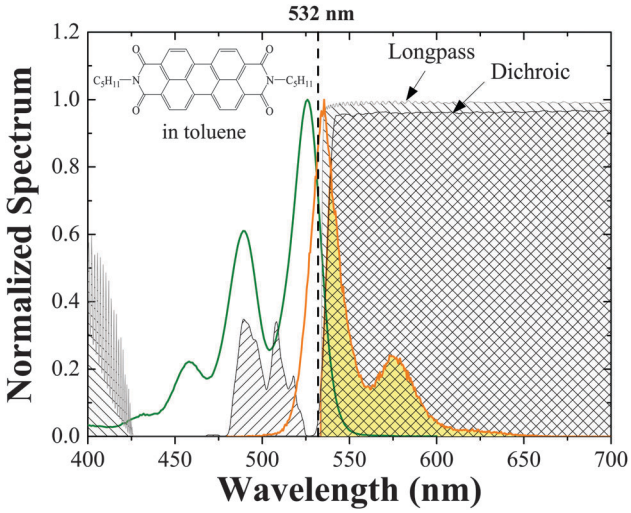

Fig. 3 Transmission spectra of optics (dichroic mirror and longpass filter) selected for a set-up using 532 nm excitation and the fluorescent probe *N,N′*-dipentyl-3,4,9,10-perylenedicarboximide (pPDI, with structure shown in inset). Absorption (green solid line) and emission (orange solid line) spectra of pPDI in toluene are shown, as is the transmission spectra of a dichroic mirror (Semrock, LPD01-532RU) and longpass filter (Semrock, LP03-532RU) appropriate for detecting fluorescence from this probe. The yellow filled area represents the portion of the fluorescent signal transmitted to the detector. For the depicted setup, $\approx 40\%$ of the emitted signal is lost to spectral filtering.

III. Data analysis overview

The general approach to studying rotational motion of single molecule probes in supercooled liquids begins with fluorescence intensity measurements of single molecule probes in two orthogonal polarizations. These intensities are typically combined into a linear dichroism. Analysis of individual linear dichroism trajectories in time, autocorrelation functions of individual linear dichroisms, and distributions of variables obtained from analysis of many such autocorrelations, each provides information about a supercooled liquid that cannot be obtained from ensemble experiments.

As described in Section IIA and depicted in Fig. 2, fluorescent probes of all orientations are homogeneously excited, and fluorescence in two orthogonal polarizations is split by a polarizing beam splitter and measured simultaneously. In a confocal approach, two fluorescent intensity trajectories from a single probe are collected on two APDs while in a wide-field approach, two images are recorded simultaneously on two regions of a single CCD camera. Data collected in the wide-field configuration must be retrieved from the images, and we focus on that aspect of the data analysis of single molecule microscopy of supercooled liquids here, depicted in Fig. 4. In the wide-field approach, each frame contains fluorescence intensities of two orthogonal polarizations

for as many as several hundred molecules dispersed across the field of view. In any given image, some single molecules may not be identifiable by eye as they may be in a dark state or may have an out-of-plane orientation leading to low intensity. In order to identify all single molecule probes, it is useful to sum multiple frames before performing a feature finding procedure: this time-average of the signal increases the signal-to-noise ratio. In standard image analysis, image filters are often used to enhance signal-to-noise ratio, and this can be done here as well. Such image processing is done only in the preliminary steps, to allow for identification of single molecule probes. From this summed and filtered image (Fig. 4a), fluorescent features are identified by their brightness and size, and their positions are tabulated.

Following selection of single molecules, coordinate information is used to identify, tag, and track molecules through all frames of the movie. Intensities in the two orthogonal polarizations of each single molecule are then extracted frame by frame from the raw image data (Fig. 4b). Single molecule raw intensities ($rI_s(t)$, $rI_p(t)$) are obtained from the area of the inner circle shown in the inset of Fig. 4a, and the area between the inner and outer circles is used to extract (a space and time local) background signal for each identified molecule at each time point. The background signal is subtracted from the measured raw intensities to compensate for possible time-dependent fluctuations of the excitation light and intensity heterogeneities across the field of view. The two intensities that represent the single molecule fluorescence in each polarization are:

$$I_s(t) = rI_s(t) - B_s(t) \quad I_p(t) = rI_p(t) - B_p(t) \tag{1}$$

Both in-plane orientation angle, θ, and reduced linear dichroism, LD, can be obtained from these intensities *via*

$$\theta(t) = \tan^{-1}\left(\sqrt{I_s(t)/I_p(t)}\right) \text{ and } \mathrm{LD}(t) = \frac{I_s(t) - I_p(t)}{I_s(t) + I_p(t)} \tag{2}$$

In principle, either quantity can be used for all subsequent analysis described, though we restrict our explicit discussion to linear dichroism, as it has been more commonly used. Linear dichroism represents the in-plane projection of the probe transition dipole moment. In an ideal experiment, linear dichroism fluctuates from −1 to +1, with this range covering the full 90° angular range of a dipole fully oriented along the x to y direction. In practice, the out-of-plane component of the dipole together with the influence of the non-zero NA objective can restrict the linear dichroism fluctuations to a smaller range than expected, while imperfect background subtraction may stretch the values beyond that range.[14]

Linear dichroism fluctuations in time reveal how probe molecules rotate in the host matrix. Additional analysis of trajectories is typically facilitated through calculation of autocorrelation functions of the linear dichroism. The autocorrelation is constructed as

$$C(t) = \frac{\sum_{t'} a(t') \cdot a(t'+t)}{\sum_{t'} a(t') \cdot a(t')}, \text{ where}$$
$$a(t) = \mathrm{LD}(t) - \langle \mathrm{LD}(t) \rangle \tag{3}$$

The correlation function aids in identification and quantification of dynamic heterogeneity since its decay rate and shape yield information on average and distribution of a particular molecule's rotational dynamics, which are expected to reflect the local host dynamics around that probe. For a probe experiencing a single dynamic environment, confined for example to a region shown in Fig. 1a, an exponential form, $C(t) = \exp[-(t/\tau)]$ is expected to fit the data. For a probe experiencing a wide variety of dynamic environments, fitting $C(t)$ with an exponential function is expected to fail and a stretched exponential function, $C(t) = \exp[-(t/\tau)^{\beta}]$ with $\beta < 1$ is expected to describe the relaxation. All probes, thus, will have linear dichroism autocorrelations that can be fit by

$$C(t) = \exp[-(t/\tau)^{\beta}] \text{ with } \beta \leq 1. \tag{4}$$

For such fits, two variables are obtained, a time scale, τ, the time required for the correlation function to decay to $1/e$, and a stretching exponent, β, that captures the degree of deviation of the function from exponentiality. The rotational correlation time or characteristic relaxation time, τ_c, is calculated by integrating the autocorrelation function:

$$\tau_c = \int_{t=0}^{\infty} C(t)\mathrm{d}t = (\tau/\beta) \cdot \Gamma(1/\beta) \tag{5}$$

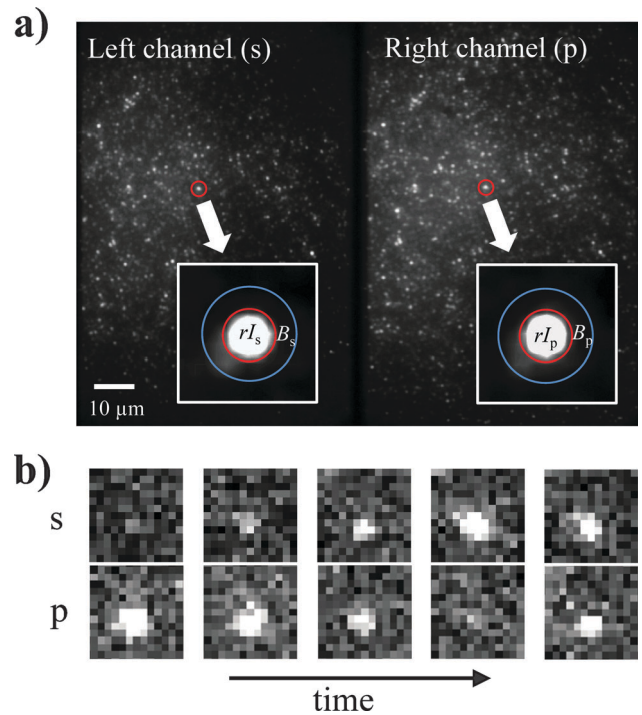

Fig. 4 (a) Summed, processed single molecule wide-field image used to identify SM probes in supercooled liquids. Left and right channels represent s and p polarization images, which are split by the Wollaston prism and focused onto the CCD camera as shown in Fig. 2. Insets are zoomed in images of a single molecule, and circles are drawn to indicate where the raw intensities of signal (rI_s, rI_p) and background (B_s, B_p) are extracted. Both signal and background intensities are extracted from unprocessed frames for individual molecules. (b) Unprocessed, time-sequenced frames of a typical single molecule in the two channels.

Thus, τ_c contains information about both how fast the correlation function decays (τ) and the variation in probe speed as it does so (β). Knowledge of two of these three variables – τ, β, and τ_c – determines the third and characterizes the rotational behavior of the molecule. In practice, β and τ_c are usually examined; τ_c is preferred to τ as the integration procedure makes it less sensitive to noise than τ.

IV. Characterizing dynamic heterogeneity

Once the linear dichroism trajectories of many single molecule probes in a supercooled liquid have been obtained, a large amount of data is available for analysis. In this section, we describe approaches that have been used to characterize dynamic heterogeneity in supercooled liquids from single molecule probe linear dichroism trajectories. Fig. 5 provides an overview of information available from single molecule rotational measurements.

Linear dichroism trajectories provide the most fine-grained information available from single molecule measurements of rotational motion. These trajectories reveal information on the character of single molecule probe rotation, including whether the probes display rotations primarily through small angular displacements or sporadic large angular jumps. A visual inspection of the trajectories may also provide clues about the nature of dynamic heterogeneity in the supercooled liquid. Two probe molecules exhibiting differences in rotational relaxation time that differ by a decade would be identifiable by eye. Similarly, a single probe molecule that exhibits a change of rotational correlation time of a factor of ten – if such a change persists for a number of probe rotations – would also be identifiable by eye. In the limiting case depicted in Fig. 1a, linear dichroism trajectories that are distinct across single molecules would be evident, but no changes in time for given probes would be seen. In the limiting case depicted in Fig. 1b, linear dichroism trajectories of particular molecules would look very similar to each other and may reveal obvious regions of distinct dynamics within each trajectory.

Analysis of linear dichroism trajectories of single molecule probes in supercooled liquids has shown both small angle diffusion and relaxation through large angular jumps, with the former described more commonly in small molecule supercooled liquids and the latter more evident in polymer samples.[10–12,15,16,19,20] From single molecule linear dichroism trajectories collected in a given supercooled sample, some differences in overall relaxation time scale have been identified through visual inspection and described, as have some changes in dynamics within a given trajectory.[14] In general, however, differences in dynamics across and within trajectories have been subtle, and autocorrelation analysis has been employed to further discriminate differences in dynamical behavior.

As described in Section III, constructing an autocorrelation of an individual linear dichroism trajectory yields a decay time, τ, a stretching exponent, β, and a characteristic rotational correlation time, τ_c, that describe the molecule's rotational behavior. Collecting these quantities across molecules forms the bulk of data typically presented in single molecule studies of supercooled liquids. Assessing large numbers of single molecules is

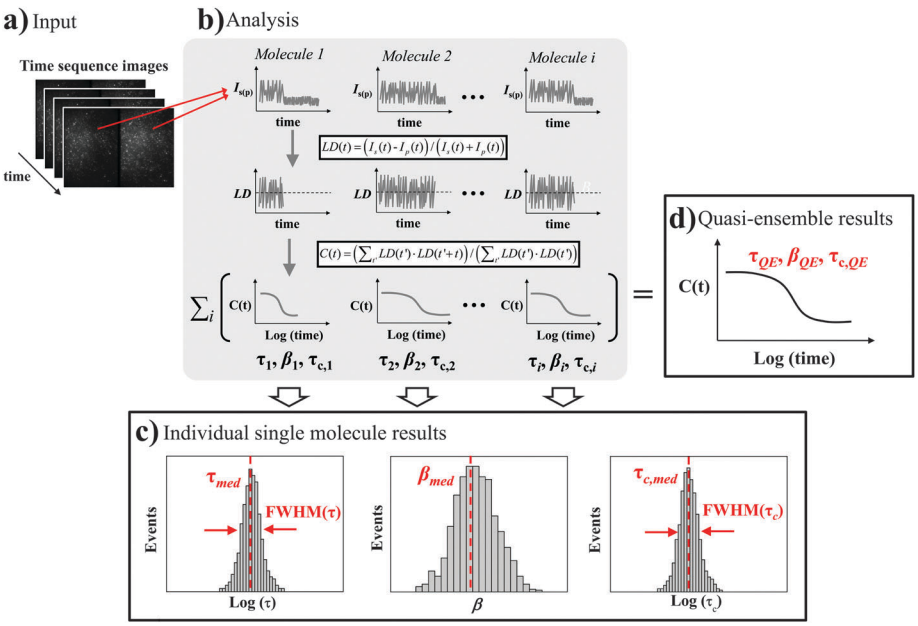

Fig. 5 Illustration of information available from single molecule rotational measurements. (a) Extraction of time-dependent intensity trajectories ($I_s(t)$, $I_p(t)$) from time-sequenced images as would be obtained from a wide-field approach that collects data from a few hundred molecules simultaneously. (b) Calculation of linear dichroism trajectories (LD(t)) from the intensity trajectories is followed by the construction of linear dichroism autocorrelation functions, $C(t)$. Autocorrelation data of each trajectory is fit to a stretched exponential function, resulting in relaxation information (τ, β, and τ_c) for each single molecule. (c) Data collected from many single molecules provide statistical information such as distribution shape, median value, and width (shown here are τ_{med}, β_{med}, $\tau_{c,med}$, FWHM(τ), FWHM(τ_c)). (d) A quasi-ensemble autocorrelation constructed from adding individual single molecule autocorrelations yields additional information on the ensemble's behavior and provides τ_{QE}, β_{QE}, and $\tau_{c,QE}$.

useful in understanding the diversity of dynamic environments within a supercooled liquid and identifying potentially rare or fleeting environments. Obtaining data from statistically significant numbers of individual single molecules also allows reconstruction of observables as they would be reflected by ensemble experiments. Comparing single molecule results to ensemble results is an important step in validating the single molecule approach and in clarifying conclusions drawn from observations in ensemble studies. There are several ways to reconstruct ensembles from single molecule experiments, and the choice of how to do so may depend on the information desired. We focus on the variables typically obtained from linear dichroism autocorrelations – τ, β, and τ_c – all of which are also available from ensemble experiments. One way to reconstruct an ensemble from single molecule measurements is to accumulate distributions of these variables from many individual single molecule linear dichroism autocorrelations and extract a value that characterizes the average of that distribution (Fig. 5c). Since the distributions of these variables are not necessarily symmetric, median rather than mean values have typically been used for comparison with values obtained from bulk experiments, and we denote those as τ_{med}, β_{med}, and $\tau_{c,med}$. A second approach to reconstructing the ensemble is averaging individual autocorrelations into a single autocorrelation, which we term a quasi-ensemble autocorrelation, ACF_{QE}. The ACF_{QE} is fit to a stretched exponential function and returns quasi-ensemble results τ_{QE}, β_{QE}, and $\tau_{c,QE}$ (Fig. 5d). A third method – which to the best of our knowledge has not been used in published work – assembles individual linear dichroism traces into a single long linear dichroism trajectory, constructs a single autocorrelation and extracts the variables of interest. This is expected to return the same values as the quasi-ensemble approach of adding the autocorrelations.

Regardless of degree and details of dynamic heterogeneity, $\tau_{c,med}$ and $\tau_{c,QE}$ values are expected to be the same, and either can be used to validate the single molecule approach. Because supercooled liquids are so dynamically sensitive to changes in temperature, a common test of the validity of single molecule experiments assesses the temperature dependence of probe dynamics through $\tau_{c,med}$ or $\tau_{c,QE}$. These dynamics are expected to follow the temperature dependence of the long time scale, structural or α-relaxation dynamics of the host as measured through either probe-free or probe-bearing ensemble measurements. In many single molecule studies in supercooled liquids, the temperature dependence obtained from a reconstructed ensemble of probes has been shown to follow the temperature dependence of the host dynamics, typically through comparison to $\tau_{c,med}$ (Fig. 6).[8,9,15,17–19,23] We note that this result is necessary but insufficient to prove that the probe is not performing significant perturbation of the host, that the ensemble sampled is fully representative of the host, that sufficient numbers of probe molecules have been analyzed, and that temperature control of the sample is adequate.

Access to $\tau_{c,med}$ implies that a distribution of τ_c values has been obtained from many individual single molecules. The shape of this distribution holds information not attainable from bulk experiments. In an ideal case of a sufficiently photostable probe that is of the same size as the host molecules comprising the system, the τ_c distribution will differ substantially for the limiting cases shown in Fig. 1a and b. For very long lived distinct environments (Fig. 1a), the full range of τ_c values present in the host will be represented, and a wide distribution of τ_c values, reflecting the native heterogeneity of the host, would be measured. For short-lived heterogeneity, a delta function at $\tau_{c,med}$ would be expected. Single molecule measurements – with distributions constructed from up to $\approx$1000 single molecule probes – have yielded distributions that are well fit by Gaussian functions in log time.[8,17,18,23] On a linear scale, these distributions have long time tails. This type of distribution is consistent with alterations in dynamics in the supercooled liquid being an activated process involving a Gaussian distribution of energy barriers.[37] The breadth of the measured τ_c distributions has been characterized by full width at half maximum (FWHM), with reported FWHM of τ_c distributions ranging from 0.2 to 1.0.[8,17,18,23] A FWHM of 1.0 reflects a distribution in which 67% of the molecules exhibit relaxation times within a decade faster or slower than $\tau_{c,med}$. Despite complications in interpretation that exert competing forces – finite probe photostability tends to widen distributions while large probe size tends to narrow them (see Section V) – the presence of τ_c distributions of substantial width argues against the existence of the limiting case depicted in Fig 1b. Whether the distribution of dynamic environments in the host measured reflects the *full* distribution remains an open question.

Beyond using τ_c distributions to provide a basic assessment of whether distinct environments within supercooled liquids persist for relatively long times, analyzing how this distribution

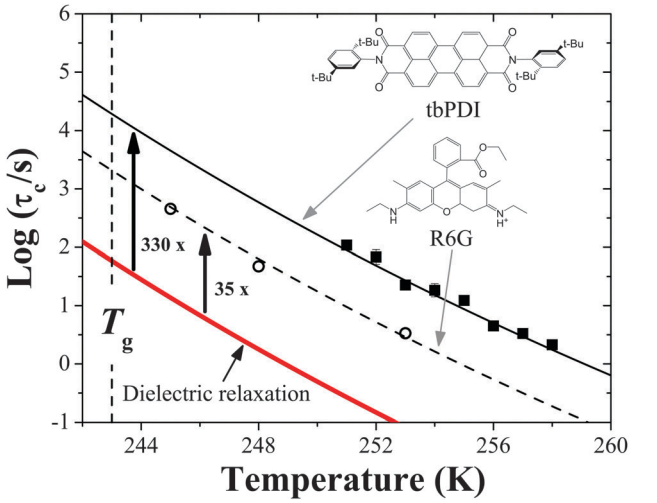

Fig. 6 Temperature dependence of probe rotation in *o*-terphenyl for *N,N′*-bis(2,5-*tert*-butylphenyl)-3,4,9,10-perylenedicarboximide (*tb*PDI, solid squares)[23] and R6G (open circles)[9] measured in single molecule experiments. Error bars on the solid squares represent the standard deviation of measurements reported in ref. 23. The solid red line represents the temperature dependence of neat *o*-terphenyl from dielectric relaxation.[43] The dashed and solid black lines are vertical shifts of the dielectric line. Dynamics of probe rotation follows that of the host, with relaxation time shifted to longer timescales according to the relative size of the probe and host. Inset shows the molecular structures of *tb*PDI and R6G.

changes as a function of temperature within a given host as well as across hosts can answer fundamental questions about the nature of the glass transition. Analyzing τ_c distributions as a function of temperature is of interest because it has been suggested that degree of dynamic heterogeneity changes as a function of temperature, and ensemble measurements in which β values vary with temperature support this view. However, other experiments in supercooled liquids show robust time–temperature superposition, in which a temperature dependent quantity known at one temperature can be used to predict that at another with a simple shift in time scale. Time–temperature superposition suggests that the degree of dynamic heterogeneity is constant in the glassy regime.[38] Thus far, single molecule experiments have not yielded fully consistent results on this point: no trend in FWHM of single molecule τ_c distributions was found in glycerol in the temperature range of 1.04–1.12 T_g or in *o*-terphenyl at 1.03–1.06 T_g.[17,23] However, others did find an apparent increase in the FWHM of single molecule τ_c distributions in the same temperature range for glycerol and in a lower temperature range, closer to T_g, for *o*-terphenyl.[8,9]

Investigating τ_c distributions as a function of supercooled liquid is also of interest. It has been proposed that higher fragility liquids, those with greater changes of viscosity as a function of temperature near T_g, may exhibit a greater degree of dynamic heterogeneity than low fragility glass formers.[1,5] Single molecule investigations have provided some evidence that probe τ_c distributions in *o*-terphenyl, a prototypical fragile glass former, and glycerol, with lower fragility, are differently shaped. While $\log(\tau_c)$ distributions in both glycerol and *o*-terphenyl are rather well fit by Gaussian curves, those in glycerol are somewhat more peaked and are equally well fit by Lorentzian curves.[17,23] Additionally, FWHM of the distributions in *o*-terphenyl appear broader than those in glycerol.[23]

In addition to analysis of τ_c distributions, τ distributions may provide additional insight. For the limiting case depicted in Fig. 1a, τ_c and τ distributions will be identical, while they will differ in the limiting case depicted in Fig. 1b. Since knowing any two of the three variables τ, β, and τ_c determines the third, this information can be equally well assessed by studying the β distribution. β distributions are particularly interesting since unlike τ_c, where $\tau_{c,med}$ and $\tau_{c,QE}$ are expected to be the same, β_{med} and β_{QE} may not be. For the case depicted by Fig. 1b, $\beta_{med} = \beta_{QE} < 1$, both of which would be equal to those of the ensemble measurements. However, in the case of long-lived heterogeneity shown in Fig. 1a, $\beta_{med} = 1$ and $\beta_{QE} < 1$, equal to that of ensemble measurement. In the limiting cases described, both β distributions would be expected to be delta functions, albeit at quite different values. Thus far, β_{med}, β_{QE}, and/or β distributions have been reported for single molecule measurements in *o*-terphenyl, glycerol, and several polymers.[9,10,13,17–19,23] In the cases in which both β_{med} and β_{QE} were reported, β_{med} was higher than β_{QE} in all cases. This result – albeit subject to uncertainties described below – is suggestive of a situation between those depicted in Fig. 1a and b, as shown in Fig. 1c.

V. Challenges to characterizing dynamic heterogeneity

In Section IV, we described how linear dichroism trajectories, autocorrelations of linear dichroism trajectories, distributions of observables obtained from these autocorrelations, and quasi-ensemble autocorrelation reconstructions can be used to characterize dynamic heterogeneity from single molecule experiments in supercooled liquids. In particular, investigating the extent to which long-lived distinct environments exist in a given supercooled liquid as a function of temperature as well as between different supercooled liquids is an accessible goal with the experiments and analysis thus far described. In practice, as introduced in Section IIE, there are challenges and limitations in interpreting linear dichroism autocorrelations and associated quantities, related primarily to probe photo-instability and probe size.

A. Probe photostability and data interpretation

The effects of probe photo-instability have been discussed in some detail in a recent review and therefore are covered only briefly here.[24] The variables obtained from a linear dichroism autocorrelation – τ, β, and τ_c, – may not be accurate if the trajectory from which the autocorrelation is constructed is too short. Indeed, information about dynamic heterogeneity may be overwhelmed by effects from time-limited trajectories, particularly for trajectories <100 τ_c and for systems with limited native heterogeneities.[36] Numerical simulations of homogeneously rotating particles (with a given $\tau_c = \tau$ and $\beta = 1$) show that distributions of extracted τ_c and β get wider with decreasing trajectory length.[24,35] Median values of these distributions may also change with trajectory length.[14,36] Thus, for single molecule probes with short trajectories, non-exponential decay of the relaxation does not necessarily point to probe exploration of various dynamic environments. Similarly, the presence of a relatively wide distribution of β values for an ensemble of single molecule probes in a supercooled liquid does not necessarily eliminate the possibility of either limiting case depicted in Fig. 1. The complications inherent in interpreting autocorrelations obtained from short trajectories also limit the ability to make time-local judgments about the rotational relaxations of a given probe from autocorrelations constructed from short portions of its linear dichroism trajectory.[9,10,12,14,17]

To date, published work on single molecule rotations in supercooled liquids has reported trajectories ranging from 10 to 1500 times the probe rotational correlation time, τ_c. To allow for straightforward interpretation, every effort should be made to collect trajectories of at least 100 τ_c. This should be an important criterion in probe choice and experimental setup, informing choice of optical configuration, balancing excitation power with time averaging in data collection, and balancing the sampling rate with trajectory length. In cases in which sufficiently long trajectories are not accessible, results from simulations should be used to guide decoupling effects from short trajectories from those due to dynamic heterogeneity.

B. Probe size and data interpretation

Given the fact that limited probe photostability complicates interpretation of single molecule reports of dynamic heterogeneity, more photostable entities than small molecule fluorophores – such as quantum dots – may be attractive alternatives. However, as introduced in Section IIE, probe size is another aspect that critically influences experimental ability to delineate dynamic heterogeneity in supercooled liquids. Probes need to be large enough to reflect host dynamics but not so large as to average over them. Indeed, if a probe is larger than regions of distinct dynamics in the host, the probe cannot report on those distinct environments, instead providing an average relaxation time of the regions it spans. Similarly, if probes rotate slowly compared to the time scales on which distinct environmental environments of the host randomize, these probes cannot report these changes.

As described in Section IV and shown in Fig. 6, demonstrating that $\tau_{c,med}$ values from single molecule probes follow the temperature dependence of the host viscosity validates that the probe samples the dynamics of host structural relaxation. Such measurements also return the rotational relaxation rate of the probe relative to that of the host. In all cases of single molecule rotational measurements in supercooled liquids thus far, probe τ_c has been more than an order of magnitude longer than host relaxation time (see, for example, Fig. 6). Probe rotations are slower than host relaxations because probe molecules are typically larger than the host molecules in organic glass formers and than the local environment governing structural relaxation in polymers. This size difference is dictated largely by photophysical requirements of the probe and purity requirements of the host. The way in which single molecule measurements may be affected by the presence of large and/or slow probes can be understood through comparison with probe-bearing ensemble experiments as well as through single molecule experiments done with a series of probes. Probe-bearing ensemble fluorescence experiments can be performed with a wider range of probes than single molecule measurements because probe photophysical requirements are less restrictive in these experiments where at least 1000 – and often orders of magnitude more – probes are averaged in a given measurement. Such ensemble measurements have shown that stretching exponent depends on probe size.[39–41]

Fig. 7a illustrates how stretching exponents as measured in rotational relaxation experiments change with size of the probe relative to that of the host for different probes in *o*-terphenyl. It is generally assumed that probe molecular weight and physical volume will track with probe rotational correlation time; however, due to variable interactions between host and probe, probe size and probe relaxation time in a particular host are not always monotonically related, as has been noted in a recent single molecule paper.[17] Despite this, molecular weight is a reasonable parameter with which to characterize probe size and relaxation rate. In Fig. 7a, stretching exponents from a variety of experiments in *o*-terphenyl are presented: β of neat *o*-terphenyl obtained from dielectric relaxation measurements,[42,43] β obtained from ensemble average photobleaching measurements,[39,44] and β_{QE} and β_{med} from single molecule measurements are shown.[9,23]

As the size of the probe increases, the stretching exponent approaches unity. This suggests that the high molecular weight probes are not reporting dynamic heterogeneity of the host, likely because they are averaging in space and/or time over the dynamics of interest. We note that the relatively large β_{QE} values obtained in these single molecule experiments stand in contrast to the breadth of the distribution of τ_c values obtained in these same experiments, which do suggest the probes are reporting dynamic heterogeneity in the host. While this juxtaposition is

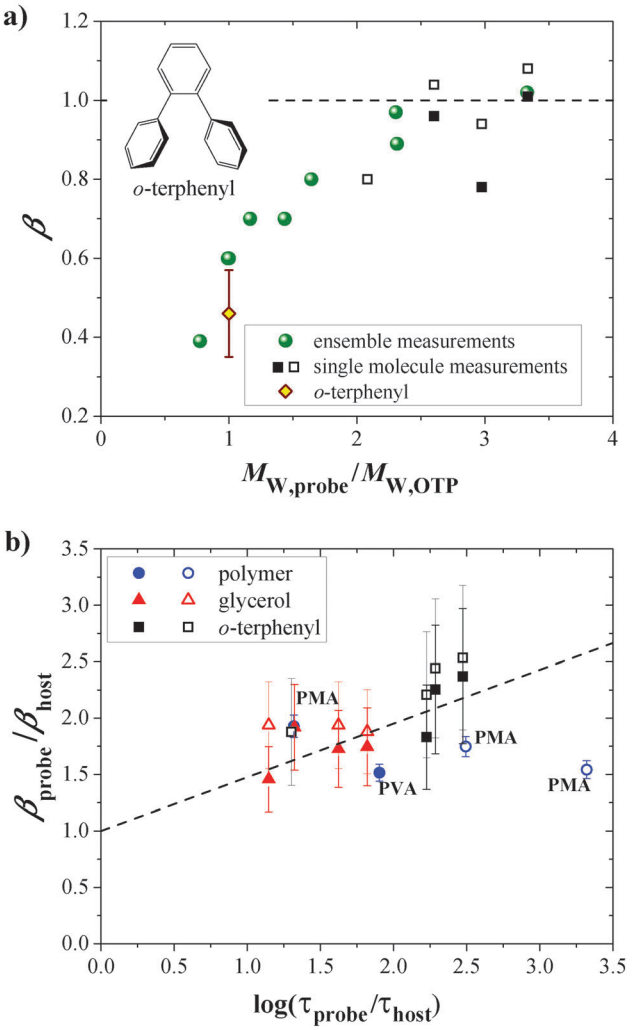

Fig. 7 Probe size dependence of the stretching exponent β. (a) Comparison of probe β values from bulk ensemble measurements (green circles)[39] and SM measurements (open squares, β_{med}; filled squares, β_{QE})[9,23] in *o*-terphenyl as a function of molecular weight of the probe relative to that of *o*-terphenyl. The diamond represents *o*-terphenyl measurements from probe-free experiments, with the error bar indicating the standard deviation of values reported.[42,43] Inset shows the molecular structure of *o*-terphenyl. (b) Dependence of scaled β values ($\beta_{probe}/\beta_{host}$) on the relative rate of probe and host relaxations (τ_{probe}/τ_{host}) for SM measurements from both low molecular weight (*o*-terphenyl, glycerol)[8,9,17,23] and polymeric (PMA, poly(methyl acrylate); PVA, poly(vinyl acetate))[10,13,18,19] glass formers. Open symbols are reported values of β_{med} and solid symbols are those of β_{QE}, as in (a). Host β and τ values are taken from a variety of reports as cited in the text, and error bars are set, as in (a), by standard deviation of host β from those reports. The dashed line is a guide to the eye.

not yet fully understood, it may be related to competing effects of limited trajectory length and probe averaging, which manifest differently in τ_c distribution than in β_{QE}.[36]

Two intriguing observations from the single molecule results are evident in Fig. 7a. First, β_{QE} is consistently lower than β_{med}, suggesting a picture of dynamic heterogeneity that may lie closer to that depicted in Fig. 1a than Fig. 1b. Second, one probe displays β_{QE} and β_{med} smaller than would be expected from the overall trend shown in Fig. 7a. This PDI probe exhibits a τ_c smaller than that of a similar PDI probe with higher molecular weight. A similar set of probes was found to display analogous behavior in glycerol, with increase in β more robustly tracking increase in probe τ_c than increase in probe molecular weight.[17] This finding suggests that temporal, rather than spatial, averaging is most important in increasing β values relative to that measured in probe-free hosts.[17,23]

Because of the fact that molecular weight and relaxation time do not always track each other, if probe relaxation time is more important in setting β than probe size, the relationship between probe speed and β should be more robust than that shown in Fig. 7a. Fig. 7b shows how scaled β varies with scaled τ_c for all single molecule measurements for which this information is available.[8–10,13,17–19,23] Error bars reflect variations in the reported ensemble β values.[1,42,43,45–48] In cases where multiple values of T_g have been reported, reduced temperature was used when calculating the relative rate of relaxation, τ_{probe}/τ_{host}. Fitting these data to a line suggests that β_{QE} will reproduce probe-free measurements if the relaxation time of the probe equals that of the host. However, for measurements in which β_{med} and β_{QE} are available, the former is always larger, suggesting that a higher stretching exponent will be returned even for probes exhibiting the same relaxation rate of the probe. The discrepancy between β_{med} and β_{QE} obtained from single molecule experiments for a probe that exhibits the same relaxation time as the host can be interpreted as the degree of dynamic heterogeneity in the probed supercooled liquid attributable to long-lived distinct dynamic environments such as those depicted in Fig. 1a.

VI. Conclusions and prospects

While all single molecule experiments have strict probe requirements, for straightforwardly detailing dynamic heterogeneity in supercooled liquids the requirements are even more restrictive. Analysis of accumulated single molecule data and comparison to ensemble experiments argue that all efforts should be made to use single molecule probes that (1) yield trajectories >100 τ_c, long enough to return a reproducibly exponential decay in the absence of dynamic heterogeneity and (2) demonstrate a β_{QE} value that is similar to that of the probe-free host. For such probe–host pairs, single molecule fluorescence microscopy can provide a precise picture of heterogeneities in the supercooled liquid, reporting the full breadth of distinct dynamic environments and how they change over time. While we reiterate that long-lived probes of similar size and rotational relaxation time to the host of interest provide the best opportunity to straightforwardly report on dynamic heterogeneity in supercooled systems, single molecule experiments with current probe–host pairs can provide significant insight into length scales and time scales of dynamic heterogeneity in supercooled liquids as well as detail how the degree of dynamic heterogeneity varies with temperature and across glass formers.

Single molecule microscopy – both with ideal probe–host pairs as well as with series of probes in given hosts – can go beyond the analysis of variables that emerge from the rotational relaxation measurements described here. For example, single molecule microscopy can be utilized to clarify the origin of the breakdown of Stokes–Einstein (SE) behavior in supercooled liquids, one of the most interesting questions in the field of glassy dynamics and a phenomenon that is accepted to be closely linked to the presence of dynamic heterogeneity. While the SE equation predicts that translational and rotational motions will have the same temperature dependence, bulk experiments have suggested that in many supercooled systems translational motion is enhanced relative to rotational dynamics at temperatures near T_g.[5,6] With suitable probes, single molecule experiments can establish whether SE breakdown may be a single molecule, single environment phenomenon.

Single molecule microscopy can also be used to enhance the study of emerging areas of interest in the study of supercooled liquids. Questions about how long-lived heterogeneities may be related to temperature history, crystal nucleation, and interfacial effects are all of interest and accessible using single molecule approaches.[49] Similarly, single molecule studies may clarify results from ensemble studies on glassy systems in which the degree of dynamic heterogeneity has been altered, as in ultra-stable glasses and in systems with embedded heterogeneity enhancers.[49,50]

Provided sufficient attention is given to potential challenges of interpretation, single molecule measurements can be employed to address both longstanding and emerging questions in the study of glassy physics and can unambiguously provide a more precise picture of dynamic heterogeneity in supercooled liquids than is available through other approaches.

Acknowledgements

This work was supported by the National Science Foundation under grant numbers CHE 0744322 and CHE 1213242.

References

1 R. Bohmer, K. L. Ngai, C. A. Angell and D. J. Plazek, *J. Chem. Phys.*, 1993, **99**, 4201.
2 M. D. Ediger, C. A. Angell and S. R. Nagel, *J. Phys. Chem.*, 1996, **100**, 13200.
3 E. W. Fischer, *Physica A*, 1993, **201**, 183.
4 T. Xia, L. T. Xiao and M. Orrit, *J. Phys. Chem. B*, 2009, **113**, 15724.
5 M. D. Ediger, *Annu. Rev. Phys. Chem.*, 2000, **51**, 99.
6 R. Richert, *J. Phys.: Condens. Matter*, 2002, **14**, R703.

7 F. Qi, T. El Goresy, R. Bohmer, A. Doss, G. Diezemann, G. Hinze, H. Sillescu, T. Blochowicz, C. Gainaru, E. Rossler and H. Zimmermann, *J. Chem. Phys.*, 2003, **118**, 7431.
8 R. Zondervan, F. Kulzer, G. C. G. Berkhout and M. Orrit, *Proc. Natl. Acad. Sci. U. S. A.*, 2007, **104**, 12628.
9 L. A. Deschenes and D. A. V. Bout, *J. Phys. Chem. B*, 2002, **106**, 11438.
10 A. Schob, F. Cichos, J. Schuster and C. von Borczyskowski, *Eur. Polym. J.*, 2004, **40**, 1019.
11 H. Uji-i, S. M. Melnikov, A. Deres, G. Bergamini, F. De Schryver, A. Herrmann, K. Mullen, J. Enderlein and J. Hofkens, *Polymer*, 2006, **47**, 2511.
12 A. N. Adhikari, N. A. Capurso and D. Bingemann, *J. Chem. Phys.*, 2007, **127**, 114508.
13 R. A. L. Vallee, T. Rohand, N. Boens, W. Dehaen, G. Hinze and T. Basche, *J. Chem. Phys.*, 2008, **128**, 154515.
14 S. A. Mackowiak, T. K. Herman and L. J. Kaufman, *J. Chem. Phys.*, 2009, **131**, 244513.
15 C. Y. J. Wei and D. A. Vanden Bout, *J. Phys. Chem. B*, 2009, **113**, 2253.
16 E. Braeken, G. De Cremer, P. Marsal, G. Pepe, K. Mullen and R. A. L. Vallee, *J. Am. Chem. Soc.*, 2009, **131**, 12201.
17 S. A. Mackowiak, L. M. Leone and L. J. Kaufman, *Phys. Chem. Chem. Phys.*, 2011, **13**, 1786.
18 S. Adhikari, M. Selmke and F. Cichos, *Phys. Chem. Chem. Phys.*, 2011, **13**, 1849.
19 D. Bingemann, R. M. Allen and S. W. Olesen, *J. Chem. Phys.*, 2011, **134**, 024513.
20 G. Hinze, T. Basche and R. A. L. Vallee, *Phys. Chem. Chem. Phys.*, 2011, **13**, 1813.
21 B. M. I. Flier, M. Baier, J. Huber, K. Mullen, S. Mecking, A. Zumbusch and D. Woll, *Phys. Chem. Chem. Phys.*, 2011, **13**, 1770.
22 B. M. I. Flier, M. C. Baier, J. Huber, K. Mullen, S. Mecking, A. Zumbusch and D. Woll, *J. Am. Chem. Soc.*, 2012, **134**, 480.
23 L. M. Leone and L. J. Kaufman, *J. Chem. Phys.*, 2013, **138**, 12A524.
24 L. J. Kaufman, *Annu. Rev. Phys. Chem.*, 2013, **64**, 177.
25 D. Woll, E. Braeken, A. Deres, F. C. De Schryver, H. Uji-i and J. Hofkens, *Chem. Soc. Rev.*, 2009, **38**, 313.
26 W. E. Moerner and D. P. Fromm, *Rev. Sci. Instrum.*, 2003, **74**, 3597.
27 R. E. Thompson, D. R. Larson and W. W. Webb, *Biophys. J.*, 2002, **82**, 2775.
28 X. Michalet, R. A. Colyer, G. Scalia, A. Ingargiola, R. Lin, J. E. Millaud, S. Weiss, O. H. W. Siegmund, A. S. Tremsin, J. V. Vallerga, A. Cheng, M. Levi, D. Aharoni, K. Arisaka, F. Villa, F. Guerrieri, F. Panzeri, I. Rech, A. Gulinatti, F. Zappa, M. Ghioni and S. Cova, *Philos. Trans. R. Soc. London, Ser. B*, 2013, **368**, 20120035.
29 G. Hinze, G. Diezemann and T. Basche, *Phys. Rev. Lett.*, 2004, **93**, 203001.
30 C. Y. J. Wei, Y. H. Kim, R. K. Darst, P. J. Rossky and D. A. Vanden Bout, *Phys. Rev. Lett*, 2005, **95**, 173001.
31 Q. Qin and G. B. McKenna, *J. Non-Cryst. Solids*, 2006, **352**, 2977.
32 T. K. Herman, S. A. Mackowiak and L. J. Kaufman, *Rev. Sci. Instrum.*, 2009, **80**, 016107.
33 R. Richert, *Annu. Rev. Phys. Chem.*, 2011, **62**, 65.
34 D. Bingemann, *Chem. Phys. Lett.*, 2006, **433**, 234.
35 C. Y. Lu and D. A. Vanden Bout, *J. Chem. Phys.*, 2006, **125**, 124701.
36 S. A. Mackowiak and L. J. Kaufman, *J. Phys. Chem. Lett.*, 2011, **2**, 438.
37 C. Monthus and J. P. Bouchaud, *J. Phys. A*, 1996, **29**, 3847.
38 C. A. Angell, K. L. Ngai, G. B. McKenna, P. F. McMillan and S. W. Martin, *J. Appl. Phys.*, 2000, **88**, 3113.
39 M. T. Cicerone, F. R. Blackburn and M. D. Ediger, *J. Chem. Phys.*, 1995, **102**, 471.
40 W. Huang and R. Richert, *Philos. Mag.*, 2007, **87**, 371.
41 L. M. Wang and R. Richert, *J. Chem. Phys.*, 2004, **120**, 11082.
42 F. Fujara, B. Geil, H. Sillescu and G. Fleischer, *Z. Phys. B: Condens. Matter*, 1992, **88**, 195.
43 R. Richert, *J. Chem. Phys.*, 2005, **123**, 154502.
44 K. Paeng, C. T. Powell, L. Yu and M. D. Ediger, *J. Phys. Chem. Lett.*, 2012, **3**, 2562.
45 R. Casalini, D. Fragiadakis and C. M. Roland, *Macromolecules*, 2011, **44**, 6928.
46 A. Sanchis, M. G. Prolongo, R. M. Masegosa and R. G. Rubio, *Macromolecules*, 1995, **28**, 2693.
47 K. Schroter and E. Donth, *J. Chem. Phys.*, 2000, **113**, 9101.
48 L. E. Walther, N. E. Israeloff, E. V. Russell and H. A. Gomariz, *Phys. Rev. B: Condens. Matter Mater. Phys.*, 1998, **57**, 15112.
49 M. D. Ediger and P. Harrowell, *J. Chem. Phys.*, 2012, **137**, 080901.
50 K. Ueno and C. A. Angell, *J. Phys. Chem. B*, 2011, **115**, 13994.